

LAPPEENRANNAN-LAHDEN TEKNILLINEN YLIOPISTO LUT
LAPPEENRANTA-LAHTI UNIVERSITY OF TECHNOLOGY LUT

LUT School of Energy Systems

The Department of Mechanical Engineering

Research Group of Laser Materials Processing and AM

LUT Scientific and Expertise Publications

Raportit ja selvitykset – Reports

123

Vesa Tepponen, Shahriar Afkhami, Ilkka Poutiainen

Verkostoitumisella voimaa 3D-tulostukseen (VERKOTA) -project report



LUT University
School of Energy Systems
Department of Mechanical Engineering
Laboratory of Laser and AM

Raportit ja selvitykset - Reports

Verkostoitumisella voimaa 3D-tulostukseen (VERKOTA) -project report

Lappeenranta–Lahti University of Technology LUT
Vesa Tepponen, Junior researcher, LUT
Shahriar Afkhami, Post-doctoral researcher, LUT
Ilkka Poutiainen, Head of Laser Laboratory, LUT

ISBN 978-952-335-954-3

ISSN-L 2243-3384

ISSN 2243-3384

Lappeenranta 2023

Abstract

The project strength to industrial 3D printing via networking and research, VERKOTA (Verkostoitumisella voimaa 3D-tulostukseen) is funded by the European Regional Development Fund (ERDF). This project is a partnership between LUT University (Research group of Laser Material Processing & Additive Manufacturing, and Steel Structures), and University of Turku. Several industrial partners have also joined this project to upscale the R&D activities. The project started on 1.1.2021 and continued until 31.3.2023.

The project comprised of educational events and research cases in the field of additive manufacturing (AM). Educational events were organized in the form of online webinars and a practical hands-on type of workshop, which were free to register and join. Webinars concluded a variety of presentations of present state of AM from industry experts to research and case studies conducted in LUT and UTU Universities. Practical workshop concluded basics of AM processes and design for additive manufacturing (DfAM), and an individual assignment, which comprised of designing, manufacturing, and post-processing of own AM parts from start to finish. Workshop was aimed at designers with little to no earlier experience in AM.

Research content for the project concluded various research and case studies focusing on metal AM. Studies included distinct topics in the field of material science and characterization, and design and structural optimization. Studies introduced and discussed in this report were conducted in LUT Laser processing & Additive manufacturing and Steel structures facilities.

Tiivistelmä

Verkostoitumisella voimaa 3D-tulostukseen (VERKOTA) on Euroopan aluekehitysrahaston (EAKR) rahoittama projekti. Tämä projekti on yhteistyö LUT-yliopiston (Laser Material Processing & Additive Manufacturingin ja Steel Structures -tutkimusryhmä) ja Turun yliopiston välillä. Myös useat teolliset kumppanit ovat liittyneet tähän hankkeeseen T&K-toiminnan tehostamiseksi. Hanke alkoi 1.1.2021 ja jatkui 31.3.2023 saakka.

Hanke koostui lisäävän valmistuksen (AM) alan koulutustilaisuuksista ja tutkimustapauksista. Koulutustilaisuuksia järjestettiin verkkoseminaarien ja käytännönläheisen työpajan muodossa, joihin oli vapaa rekisteröityminen ja osallistuminen. Webinaarit sisälsivät erilaisia esitelmiä AM:n teknologiasta ja nykytilasta alan asiantuntijoilta sekä LUT:n ja UTU:n yliopistoissa toteutettuja tutkimuksia ja tapaustutkimuksia. Käytännön työpaja sisälsi AM-prosessien ja lisäävän valmistuksen suunnittelun (DfAM) perusteet sekä yksilöllisen tehtävänannon, joka koostui omien AM-osien suunnittelusta, valmistuksesta ja jälkikäsittelystä alusta loppuun. Työpaja oli suunnattu suunnittelutyötä tekeville henkilöille, joilla ei ollut aiempaa kokemusta lisäävästä valmistuksesta.

Hankkeen tutkimussisältö koostui erilaisista metallien lisäävään valmistukseen keskittyvistä tutkimuksista ja tapaustutkimuksista. Tutkimuksiin sisältyi erillisiä aiheita materiaalitieteen ja karakterisoinnin sekä suunnittelun ja rakenteiden optimoinnin alalla. Tässä raportissa esitellyt ja käsitellyt tutkimukset tehtiin LUT Laser Processing & Additive manufacturing sekä Steel structures -tutkimusryhmien toimesta.

Preface

Additive manufacturing (AM), also known as 3D-printing, has fast become novel industrial grade manufacturing method worldwide. AM has shown fast improvement and rising interest in the field of research, machine/equipment development, material development and process deployment in industry and academics. AM enables many technological and environmentally sustainable advantages compared to conventional manufacturing methods, but it doesn't come without limitations and process specific disadvantages. By promoting process method related research and practical know-how, this project aims to further increase knowledge and expertise within project partners.

The project strength to industrial 3D printing via networking and research, VERKOTA (Verkostoitumisella voimaa 3D-tulostukseen) is funded by the European Regional Development Fund (ERDF). This project is a partnership between LUT University (Research group of Laser Material Processing & Additive Manufacturing, and Steel Structures), and University of Turku. Several industrial partners have also joined this project to upscale the R&D activities. The project started on 1.1.2021 and continued until 31.3.2023.

This report provides an overall view on project activities including arranged webinars, practical workshop, research, and case studies conducted for the project in the field of additive manufacturing.

Vesa Tepponen, Shahriar Afkhami, Ilkka Poutiainen

June 2023, Lappeenranta, Finland

Table of contents

Abstract.....	3
Tiivistelmä	4
Preface	5
Table of contents.....	6
1 Introduction	7
2 Educational activities.....	8
2.1 Workshop: Getting to know 3D-printing in practice	8
2.2 Project webinars	9
3 Research and case studies.....	10
3.1 Consumer product remanufacturing: Toy car gear	10
3.2 Mechanical properties and microstructure of L-PBF manufactured 316L stainless steel with laser and TIG welded joints	12
.....	12
3.3 Optimized Inconel 718 pressure vessel manufactured with laser powder bed fusion 16	
3.4 Case study: Sunrob Oy tool holder	19
3.5 Case study: Lock mechanism chamber	21
3.6 Effects of additive manufacturing parameters and post-processing on the microstructural features and mechanical properties of EOS CX	22
3.7 Notch-load interactions in L-PBF 18Ni300 and their effects on the mechanical performance of the material	25
3.8 Mechanical performance and design optimization of additively manufactured honeycombs.....	28
4 Conclusions	34
References.....	35

1 Introduction

Additive manufacturing is standardized processing method defined by ISO/ASTM 52900 to be the process of joining material layer-by-layer to form three dimensional (3D) parts typically from 3D model data. Direct comparison can be made to traditional subtractive and formative manufacturing methods, where material is either removed or formed to achieve desired geometry. Terminology for AM has become broad often regarding different process methods and equipment manufacturers own designations. Common terminology includes e.g. 3D-printing, direct digital manufacturing, rapid manufacturing and rapid prototyping among others [7].

AM comprises of seven standardized process methods: Binder jetting, directed energy deposition, material extrusion, material jetting, powder bed fusion, sheet lamination and vat photopolymerization. Each method is differentiated typically by the form of suitable material feedstock and/or binding process used to join material. Typical material forms (feedstock) include filaments, wires, liquid, powder, pellets, paste and sheet materials. Material types include variety of polymers, metals, ceramics, sand, composites, and hybrid materials among others [7].

Design for AM (DfAM) is a crucial part in taking advantage of the processing method especially in industrial grade applications. AM can offer part performance enhancing features, such as topology optimization, lattice structures and conformal channels, which often are challenging with traditional manufacturing method. Exploiting these features is key in gaining profitability through AM, while knowing the process possibilities and limitations [7].

2 Educational activities

Educational activities comprised of two webinars and a practical workshop. Webinars concluded various speakers from different companies and institutes with focus on metal AM related presentations. First webinar was arranged on November 12, 2021, and final project closing webinar on March 29, 2023. A practical metal AM related workshop was arranged during summer of 2022. Activities are presented in more detail in the following chapters.

2.1 Workshop: Getting to know 3D-printing in practice

A practical workshop regarding metal AM was arranged and aimed for design workers in industrial companies with little to no earlier experience in the field of metal AM. The workshop consisted of two contact days and carrying out an AM design assignment independently. The first contact day (31.5.2022) consisted of lectures on basics of AM, design for additive manufacturing (DfAM) and possibilities and limitations of AM, which gave the attendees tools for carrying out the individual design task. The day was concluded with a tour in LUT Laser processing & AM laboratory facilities where participants had the chance to familiarize themselves with laser powder bed fusion (L-PBF) equipment and setup. Follow up days were reserved for individual assignment, during which a remote Q&A session was held. The second contact day (31.8.2022) consisted of review and post-processing of designs works that had been printed prior to the contact day. Post-processing session and finalized parts can be seen in figure 1.



Figure 1. Post-processing and outcomes of individually designed AM parts (Gear shifter knob)

A survey was conducted for all participants after workshop was concluded. Survey questions addressed overall contentment and meaningfulness of the workshop for the participants. Survey questions and results are presented in table 1.

Table 1. VERKOTA Workshop: Getting to know 3D-printing in practice -survey results.

Grade	1	2	3	4	5	6	7	8	9	10
Q1	Did you find the workshop interesting? (1=Not at all, 10=Extremely)									
A1								1	2	1
Q2	Do you feel the workshop gave new views for your profession? (1=Not at all, 10=Absolutely)									
A2								1	2	1
Q3	Was the workshop workload appropriate? (1= Too light, 10=Too laborious)									
A3				1	2		1			
Q4	Overall satisfaction (1=Not satisfied at all, 10=Very satisfied)									
A4								2	1	1

According to questionnaire, the attendees found the workshop very interesting and its content innovative for their line of work/profession. The workload was considered appropriate and overall workshop satisfaction was good.

2.2 Project webinars

2021 webinar was held online on November 12 and consisted of VERKOTA -project introduction, University introductions of LUT and UTU, company speakers from Delva (Industrial case studies from metal 3D printing), Materflow (Plastic 3D printing in industrial production) and Andritz Savonlinna Works (Latest developments in printing of large metal parts) and a case study presentation from LUT. The closing seminar was held on March 29, 2023, with focus on various metal AM research cases regarding design, post-processing, material and part properties and simulation studies with speakers from LUT and UTU. Most of the presented topics are further introduced and discussed in the upcoming “Research and case studies” chapter of this report. Both webinars were arranged in English and were free to register and join.

3 Research and case studies

3.1 Consumer product remanufacturing: Toy car gear

Additive manufacturing is adding values to the lives of people in various means including the industrial and consumer products such as toys, hand tools, home appliances, to mention but a few. AM allows new news manufacture aesthetically and functional optimized product designs which are otherwise not possible with conventional comparable processes. AM allows also a swift and robust workflow cable of minimizing lead time and cost through reverse engineering. Examples of these are industrial machine parts and consumer products such as the examples. Reverse engineering and AM help to lighten the design process to swiften the product design of components that may be out of supply. Remanufacturing refers to the restoring damaged components by fixing or replacing them with new parts for continuous usage. AM can be used to replace broken parts of both industrial and consumer products via reverse engineering.

LUT laser and AM was approached by a customer after gaining the knowledge of the capabilities of AM to rebuild a broken gear for a consumer toy car. LUT AM through the workflow of reverse engineering for AM conducted a case study for remanufacturing the broken part to increase the service life of the toy car.

Initial thoughts of the customer included: Where can I repair this part? How fast can I get a replacement part? How much will it cost in relation to buying a new part? Is it even possible to get a new part or the spare part? Etc.?

The broken gear is shown in figure 2.



Figure 2. Original broken gear.

The working workflow used by LUT laser and AM to repair the gear for the consumer toy car as as shown in the figures 3-5. Scans of the original gear, examining of existing detailed

design information and specification for reconstructing the initial geometrical design for the three-dimensional (3D) modelling.

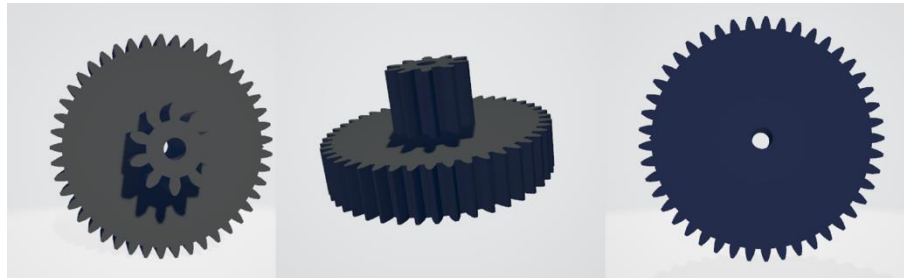


Figure 3. Scans of old gear for reconstruction or redrawing for the CAD modelling with existing design details.

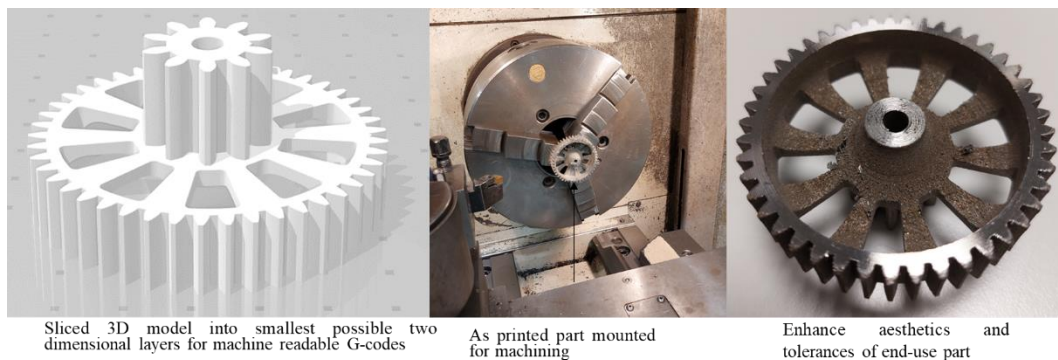


Figure 4. Representation of sliced 2D layers, as printed and machined images of gear.

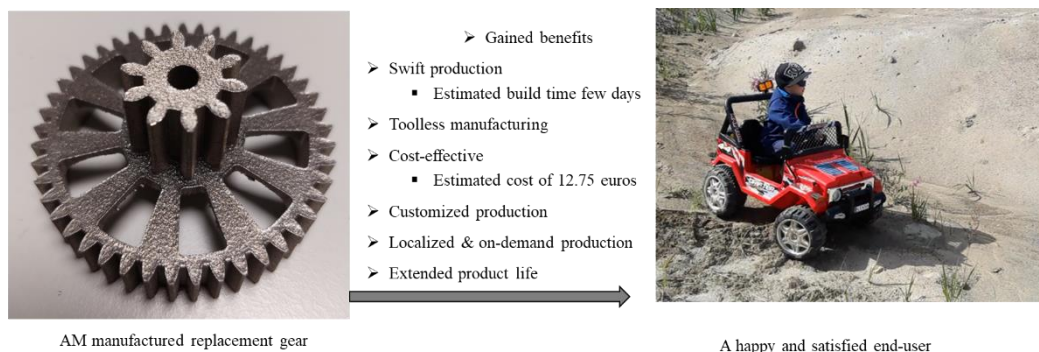


Figure 5. Summarization of case study with offered benefits of re-engineering the toy gear.

Utilization of the digital capabilities to reverse engineer existing parts can quicken product developmental times through virtual designing, validation and fine-tuning of geometry before committing to physical manufacturing. Such approach help reduces costs and saves raw material. Repairability of worn-out product assemblies directly enhances resource consumption efficiencies. The different subcategories of AM offer way to manufacture physical products as a direct replicate of virtual models referred to as the digital twin. This

approach to manufacture first-time-right products on demand. The ability to create a virtual representation of physical parts offer several advantages such as testing, validation via simulation, thereby reduce the chances of try and error with tangible material saving and replace physical storing of products with digital part inventory to be manufactured when and where needed.

3.2 Mechanical properties and microstructure of L-PBF manufactured 316L stainless steel with laser and TIG welded joints

Mechanical and microstructural properties of metal AM parts are well known and studied by this date. L-PBF manufactured metal parts can add value and functionality to existing products, but typically require suitable joining method. This research studies the mechanical and microstructural properties of L-PBF produced 316L stainless steel (SS) parts joined by laser and tungsten inert gas (TIG) welding methods. Joint types concluded butt joint, butt joint with additively manufactured root backing and lap joint with additively manufactured overlapping strip section. Root backed and lap joints were chosen to find out capabilities of L-PBF in producing prefabricated weld joint features. AM test parts were manufactured in horizontal and vertical orientations for each sample variation. Dissimilar joint samples were also prepared with conventional 316L SS welded to horizontally and vertically additively manufactured sheet parts. Principle of different sample variations can be seen in figure 6.

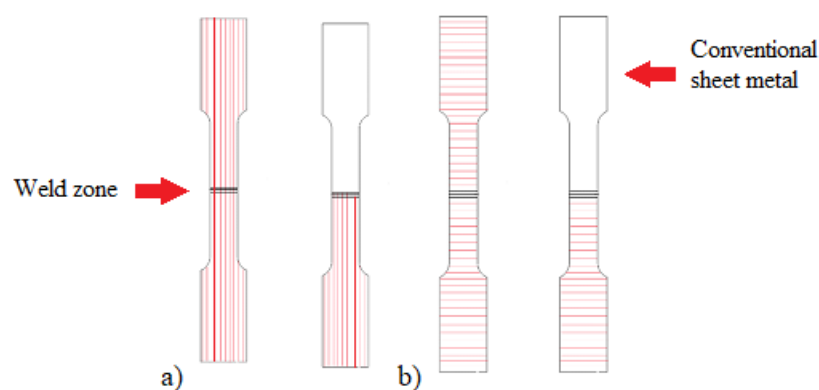


Figure 6. Sample variations: a) Vertically and b) horizontally prepared tensile test samples with L-PBF and conventional 316L SS.

Produced sheet samples were joined with robotized laser welding and manual TIG welding Utilized laser and TIG welding parameters are presented in tables X and X accordingly.

Table 2. Laser welding parameters for each joint type.

Joint	Power (kW)	Welding speed (m/min)	Defocus (mm)	Angle (Degrees)
Butt joints	5	3	0	0
Root backing	4	3	0	0
Lap joints	2	2	+20	12

Table 3. TIG welding parameters for each joint type.

Joint	Current (A)	Voltage (V)	Welding time (s)	Welding speed (cm/min)
Butt joints	140	12,5–13,3	31–32	18,8–19,4
Root backing	121	11,0–11,6	25–34	17,6–24,0
Lap joints	105	10,7–11,8	30–39	15,4–20

Tensile test results are categorized by welding method and joint type for each stress-strain plot. Sample markings abide by the following abbreviations: Weld method (L=Laser, T=TIG), AM orientation (H=Horizontal, V=Vertical) and Joint type (1=Butt joint, 2=Dissimilar butt joint), (3=Root backed butt joint, 4=Dissimilar root backed butt joint), (5=Lap joint, 6=Dissimilar lap joint). Transverse tensile test results are presented in figure 7 and table 8.

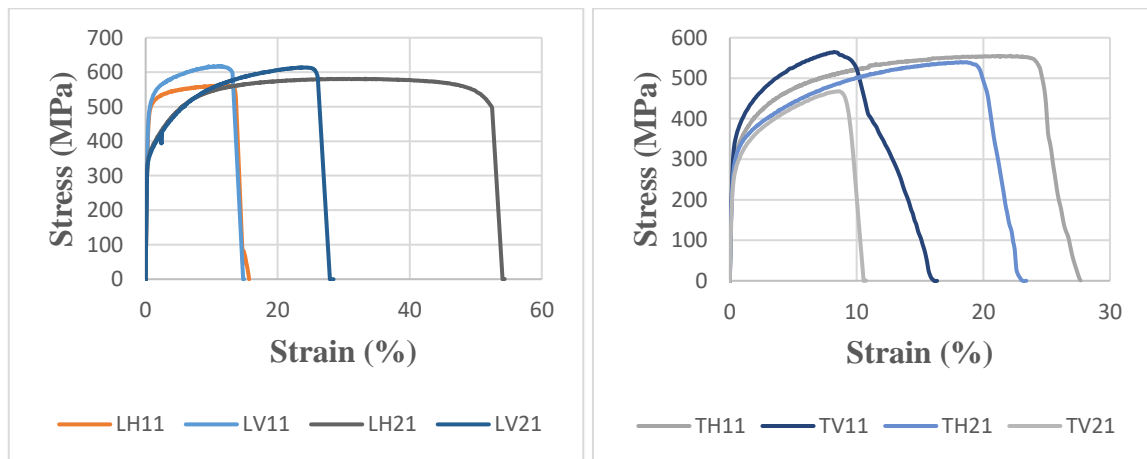


Figure 7. Tensile test stress-strain curves: Weld method (L=Laser, T=TIG), AM build orientation (H=Horizontal, V=Vertical) and Joint type (1=Butt joint, 2=Dissimilar butt joint).

Highest yield strength in laser welded samples was noted in similar joints (LH1, LV1), as dissimilar joints (LH2, LV2) showed notable strain increase with same amount of stress. Slightly higher ultimate tensile strength (UTS) value was noted with vertically manufactured samples. Higher elongation was seen in dissimilar joints, where strain was notably amounting on conventionally manufactured 316L sides. TIG welded samples showed very little variation between tensile strength values. Notably strain was amounting on the larger weld zone as compared to narrow zones produced by laser welding. Root backed joints showed identical strength properties in laser welded samples as butt joint samples, however TIG welded samples showed notable decrease in strength properties with same comparison. Subsequent visual inspection revealed that adequate welding penetration depth was not achieved with most of the root backed TIG welded samples. However, AM produced root backing and lap joint strips showed potential in adding external features for weld seams in suitable applications.

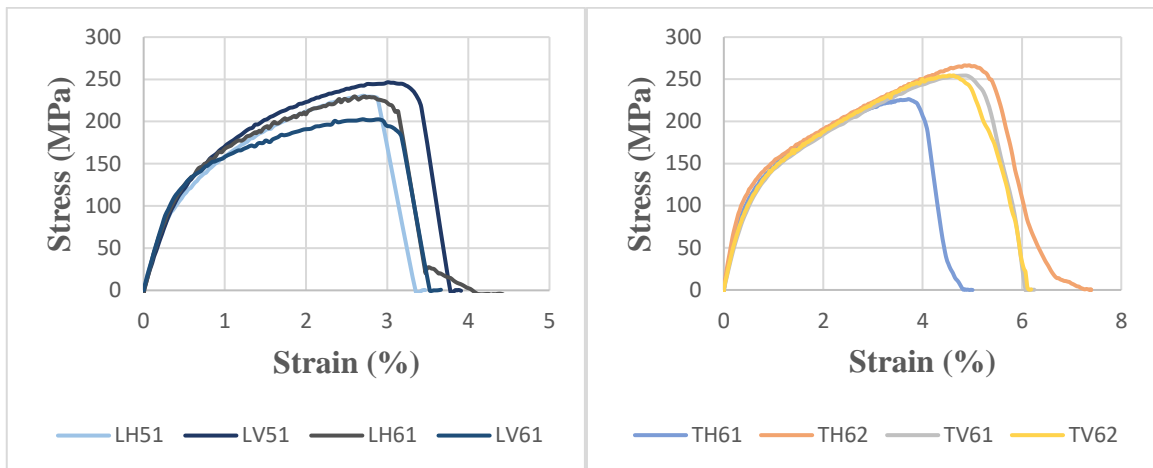


Figure 8. Tensile test stress-strain curves: Weld method (L=Laser, T=TIG), AM build orientation (H=Horizontal, V=Vertical) and Joint type (5=Lap joint, 6=Dissimilar lap joint).

Lap joint samples showed little to no divergence between tensile strength values, which was expected with the joint type, as tensile tests were carried out with non-standardized method considering lap joint testing. Mechanical properties of test samples can be seen in table 4.

Table 4. Mechanical properties of AM 316L SS welded joints.

Sample	Yield strength 0,2% (MPa)	Yield strength 2% (MPa)	Ultimate tensile strength (MPa)	Elongation (%)
LH1	297	536	563	8,3
TH1	266	405	567	22,0
LV1	305	558	622	11,1
TV1	282	451	525	8,3
LH2	296	419	581	33,3
LV2	294	412	614	23,3
TH2	248	379	560	18,3
TV2	225	361	496	8,6
LH3	296	546	589	23,5
LV3	316	567	649	16,8
TH3	293	175	372	0,4
TV3	176	79	229	0,9
LV4	294	419	644	27,1
TV4	266	397	500	7,9
LH5	61	212	219	2,7
LV5	63	223	245	3,0
LH6	66	208	219	2,6
LV6	71	191	205	2,7
TH6	64	189	246	3,7
TV6	51	186	254	4,8

Vickers hardness tests (HV5) were carried out for six different butt joint samples with adequate diversity in welding method, AM orientation and material (dis)similarity. Results are presented in table 5.

Table 5. Vickers hardness (HV5) tests along different butt joint samples. Additively manufactured 316L SS side (AM), conventional 316L SS side (CM).

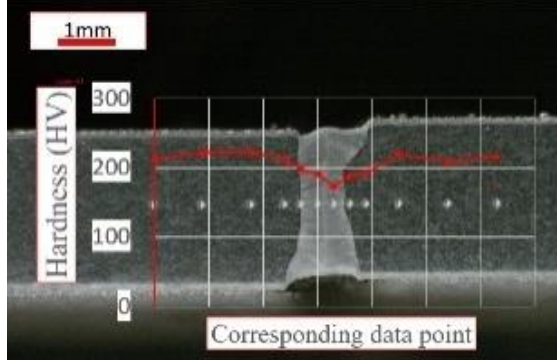
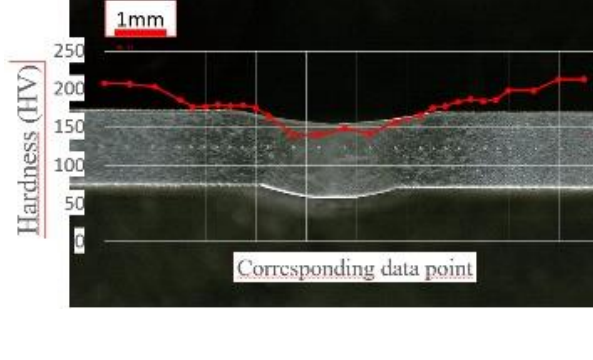
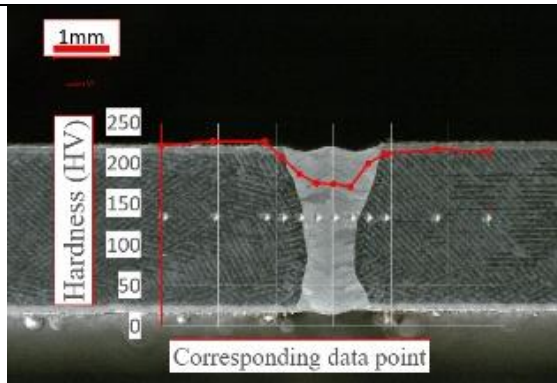
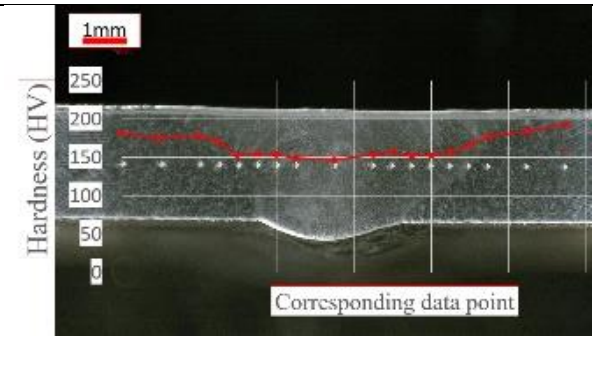
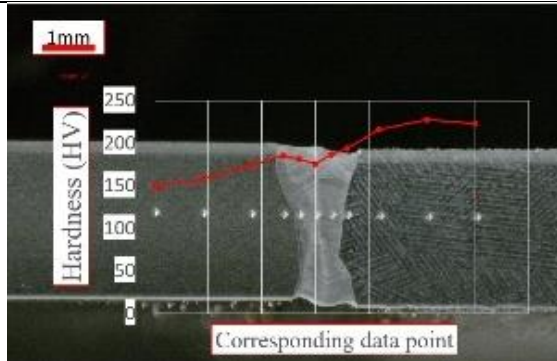
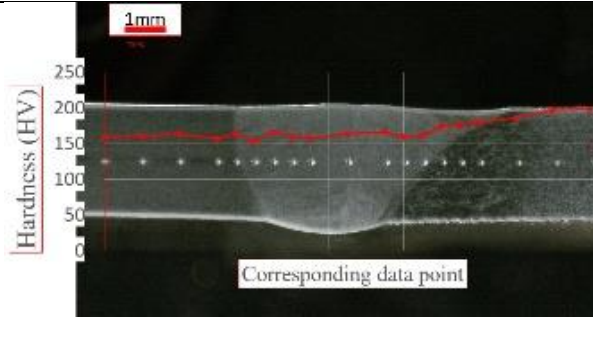





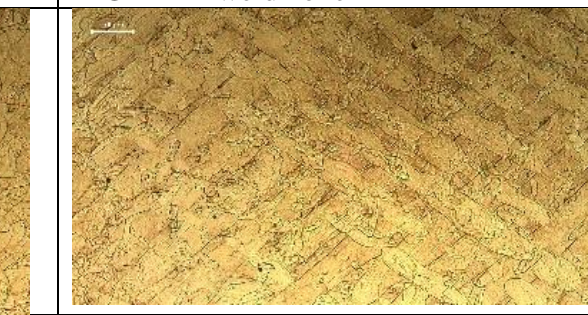
Laser weld	TIG weld
	
Horizontal orientation – AM x AM (LH1)	Horizontal orientation – AM x AM (TH1)
	
Vertical orientation – AM x AM (LV1)	Vertical orientation – AM x AM (TV1)
	
Vertical orientation – CM x AM (LV2)	Horizontal orientation – CM x AM (TH2)

Table 6. Weld zone microstructure: Additively manufactured 316L SS side (AM), conventional 316L SS side (CM).

	
Laser weld – CM weld zone	Laser weld – AM weld zone
	
TIG – CM weld zone	TIG – AM weld zone
	
AM base metal – Horizontal	AM base metal - Vertical

Notable from hardness tests (table 5) was that AM build orientation had little to no effect on achieved hardness values. However, AM base material showed notably higher hardness values compared to CM base material (AM: ~225HV, CM: ~150HV). The narrow laser weld zones achieved hardness values of approximately 175HV, while the wider TIG weld zones showed hardness values of ~150HV.

3.3 Optimized Inconel 718 pressure vessel manufactured with laser powder bed fusion

Aim of the research case was to redesign a pressure vessel with a predefined geometry (figure 9) utilizing possibilities of DfAM. Concept geometry contains non-ideal pressure vessel form with high surface to volume ratio, that can be found e.g., in heat exchangers. Objective was to exploit AM applicable structures in a linear load case of 50bar pressure and introduce few comparative design iterations based on load case FE-analysis. Boundary

condition for stress was chosen as close exceeding of heat-treated material ultimate tensile strength of 1500MPa.

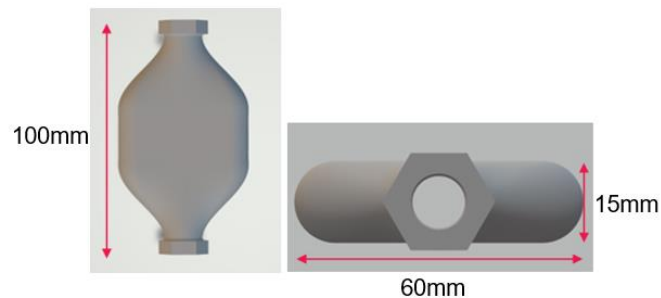


Figure 9. Pressure vessel baseline geometry and dimensions with 0.5 mm wall thickness.

Vessels were to be manufactured with L-PBF from Inconel 718, which is a nickel-based superalloy with excellent strength properties in high temperatures environments. The material is challenging to machine due to low heat conductivity, high work hardening, inherent toughness, and hardness properties. This makes AM a competitive manufacturing method for IN718 parts in complex geometry and high-performance requiring applications.

From the baseline model (0,5mm wall thickness), a benchmark model with uniform wall thickness along with 3 different optimized design iterations were generated with nTopology software. The benchmark model had 1,5mm uniform wall thickness with identical geometry as seen in figure 9. Figure 10 presents the internal lattice model, which contains two longitudinal lattice rows and has vessel wall thickness of 0,5mm. Figure 11 shows the variable shell and ribbed designs which are based on stress field analysis. Principle of the designs is that wall thickness (variable shell) or lattice thickness (ribbed) is increased in sections of the vessels where higher stress values are encountered under load according to FE-analysis.

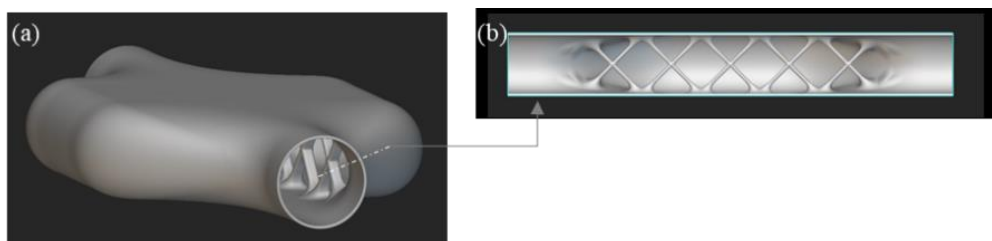


Figure 10. Internal lattice design: (a) external geometry and (b) cross-sectional view of the internal lattice.

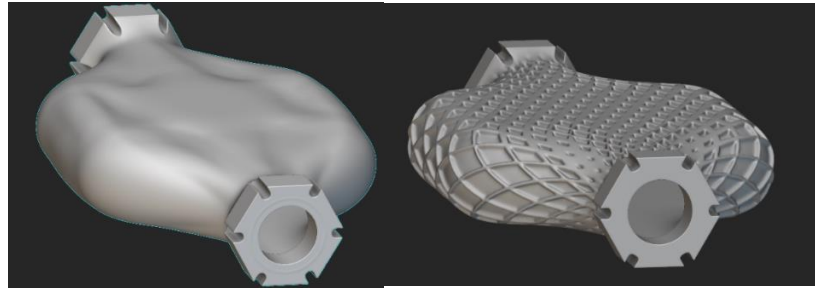


Figure 11. Variable shell thickness (left) and ribbed vessel models (right).

Pressure vessel samples were manufactured with EOS 290 L-PBF machine from EOS NickelAlloy IN718 40 μm powder with system manufacturer parameter set IN718_040_PerformanceM291 2.11. All samples were manufactured successfully, removed from build platform, and heat-treated according to EOS specifications: Step 1 involved solution annealing where parts are heated to 954 degrees Celsius (954°C) with one hour (per 25 mm of thickness) and subsequently air cooled. Second step involved ageing treatment where the parts are held at 718 degrees Celsius (718°C) for eight hours (8 hr). Then furnace is cooled to 621 degrees Celsius (621°C) for 10 hours (10 hr). Similar air cooling to earlier step. Following figures present the load case stress analysis and the matching as-built part.

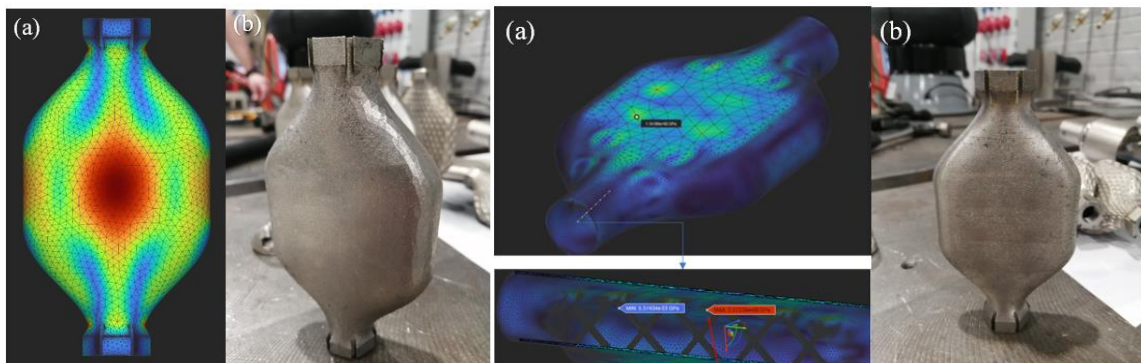


Figure 12. Representation of simulation result of stress field distribution with 50 bar pressure (a) and as-built pressure vessel (b) with uniform wall thickness (benchmark) (left) and internal lattice (right) designs.

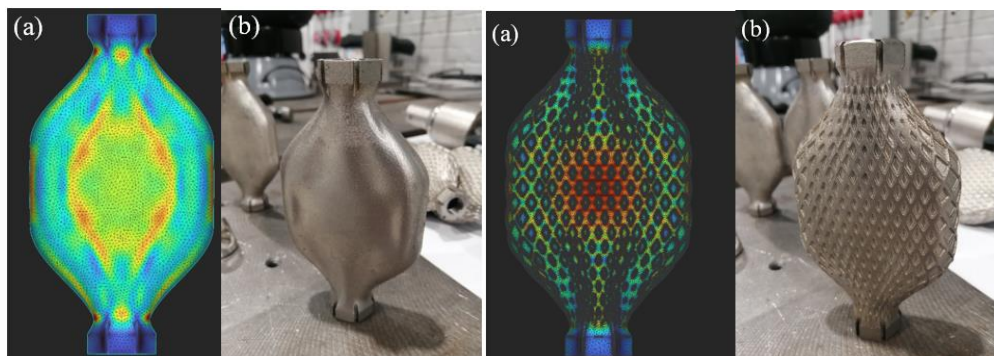


Figure 13. Representation of simulation result of surface stress field with 50bar (a) and as-built pressure vessel (b) with variable shell thickness (left) and ribbed (right) designs.

Table 7. Weight of the different vessels from simulations and weighted parts.

Design option	Weight (g)	
	Digital model	As-built part
Benchmark	160	158
Inner lattice	85,4	82
Ribbed	133	132
Variable thickness	128,9	126

In conclusion, results from this case study showed that different AM applicable structures e.g., lattice and stress field driven geometries can be utilized effectively to topologically optimize small-scale pressure vessel structures in a linear load case. Benchmark design was generated effortlessly, and the manufacturability remained excellent, however the design does not take advantage of the AM process and therefore was the heaviest iteration. Internal lattice model had the lowest weight, but applicability of such structure notably affects internal volume and material flow. Design-wise, the optimization was effortless with nTopology, which in comparison can prove challenging with traditional CAD-software. Variable shell and ribbed designs were noted to be more challenging to optimize, as number of results affecting variables increased. Furthermore, meshing of models was found problematic due to more detailed geometries, which create inconclusive stress spikes.

3.4 Case study: Sunrob Oy tool holder

Sunrob Oy gave an idea for a case study regarding a replacement part for a custom tool holder of robot they used. Part is designed be manufactured using CNC, so it didn't take advantage of AM as manufacturing method which meant it needed to be redesigned. Original part can be seen in figure 14.

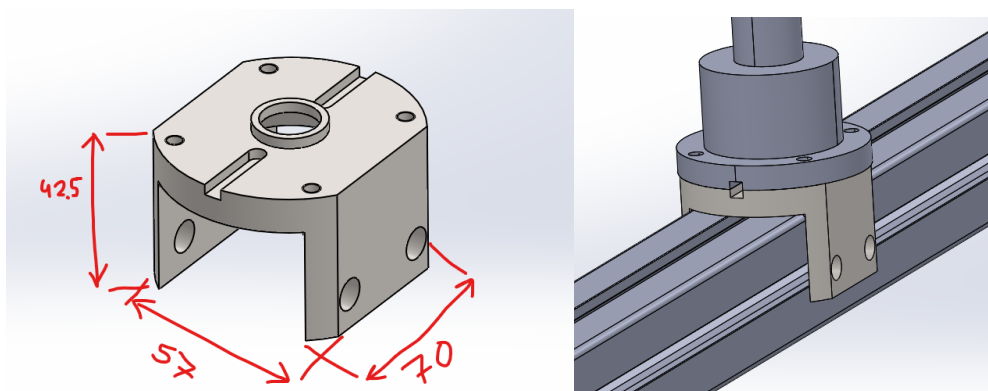


Figure 14. Sunrob tool holder geometry and attachment.

Topology optimization was used for the redesigning process with 40% mass constraint and stiffness maximization goal. Original part was simplified and lengthened to give the process more room to optimize as seen in figure 15.

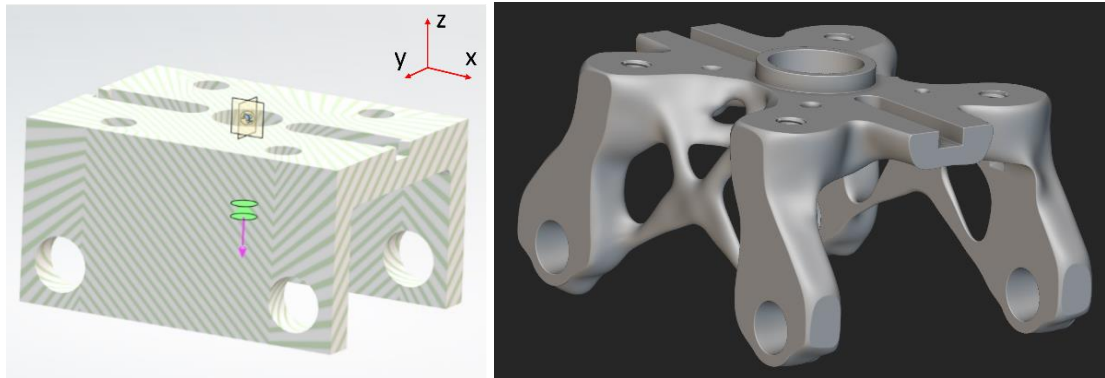


Figure 15. Tool holder design space and topological optimization.

Table 8. Loads caused by the robot arm movement along x-y-z axes.

Axis	Force (N)	Torque (Nm)
x	189,9	
y	189,9	
z	102,06	6,7

Linear forces in x and y axis were used in the lower holes and torque load on the grooves on top of the part. The size of the loads are listed on table 8. Some weight was removed by the topology optimization, but more could be done. Corners of the part still had some mass that could be reduced. Inner volume was removed to leave 1mm shell. This volume was filled with lattices. Powder would be trapped inside if the model was left like this, so triangle holes were added to the sides to let the powder out. Screw threads were also added to the holes on top of the part. Cleaning up pre-made holes is easier than cutting them to the solid material. Machining Inconel is difficult due to low thermal conductivity, high strength and work hardening of the material causing high tool wear.

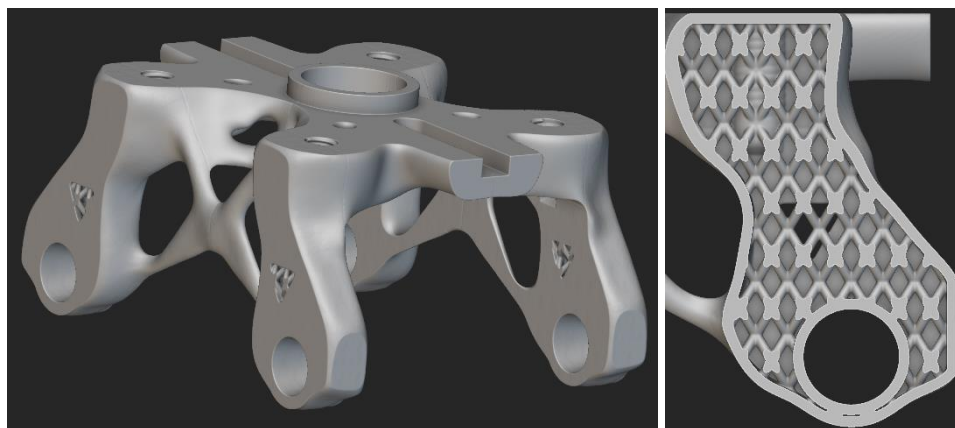


Figure 16. Final design with hollowed space with lattice structure.

Table 9. Volumes and weight reductions of different models.

	Original	Topology optimized	Shell with lattices
Volume [mm³]	44937,73	34482,11	28145,14
Weight saving	-	23,27 %	37,37 %

As seen in table 9, weight saving for topologically optimized redesign accumulated to 23% and 37% with the final version with topological optimization and internal lattice structure.

3.5 Case study: Lock mechanism chamber

A case study was conducted for a lock chamber part seen in figure 17, which houses a locking mechanism. The motivation of this study was to prepare to the possible availability problems of the parts and see if there is room for design enhancements. The original part is typically fabricated by casting or metal injection moulding (MIM). When redesigning the existing part for 3D printing the manufacturability, profitability, and requirements for post-processing plays important role when assessing the sensibility of change.



Figure 17. Original case part: Lock mechanism chamber

SolidWorks -software was used to model the original chambers defining critical geometries e.g., mechanism housing, attachment holes and outer dimensions, and adding additive manufacturability enhancing features, such as removal of material from non-critical locations and streamlined joint for attachment holes. A total of 8 parts were produced with L-PBF process from 316L stainless steel with EOS M290 in LUT Laser & AM facilities. Redesign of the lock mechanism chamber as-built parts are presented in figure 18 and produced part comparisons in figure 19.

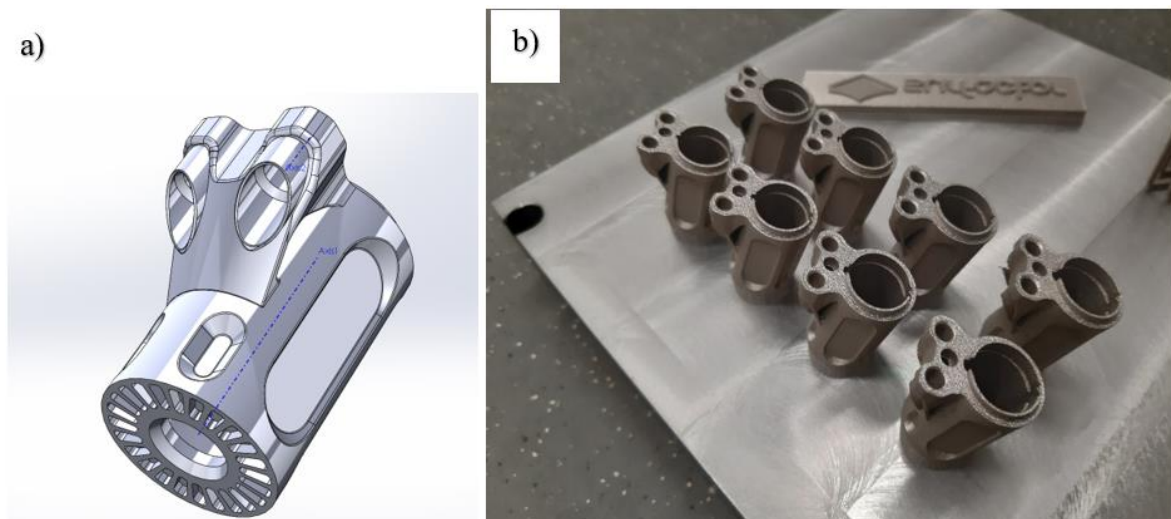


Figure 18. Chamber redesign (a) and as-built parts (b).

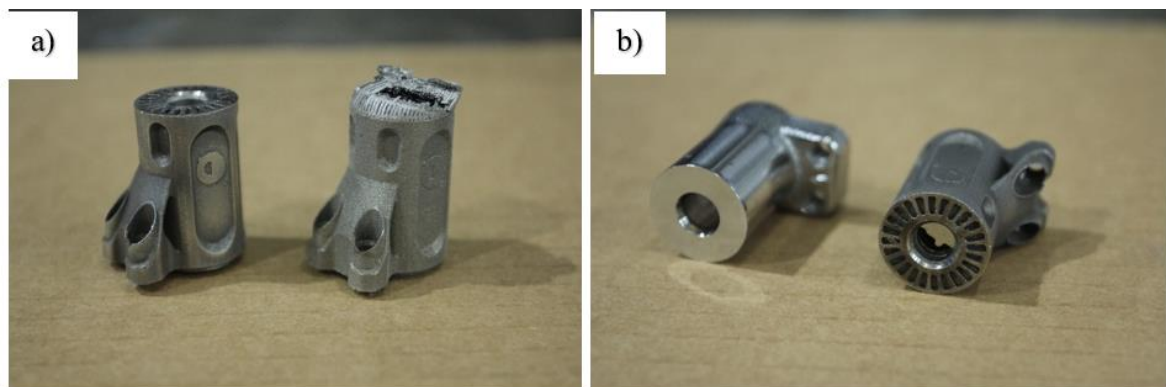


Figure 19. Post-processed chamber vs. as-built (a), original chamber vs. additively manufactured (b).

The part was post-processed and assembled by the lock smith. In the original design the inner surface is machined to get cylindrical smooth surface for the detainer discs. In the new design, the machining was not needed, and only smooth grinding was used. Material was 316L stainless steel so the step for additional coating could be ignored. For the mass production this manufacturing process is still too slow. For this reason, the price for individual part became too high. In case of sudden need of these parts a higher price can be justified.

3.6 Effects of additive manufacturing parameters and post-processing on the microstructural features and mechanical properties of EOS CX

In this study, stainless steel tool steel CX, developed by EOS, was used as the raw powder for laser-powder bed fusion (L-PBF) to investigate the effects of build orientation (as an additive manufacturing parameter), heat treatment, and mechanical machining (as post-processing methods) on the microstructure, residual stress, notch toughness, quasi-static mechanical properties, and high-cycle fatigue performance of the additively manufactured

metal. Also, using bending after L-PBF to impose tensile and compressive residual stress in samples, the influence of residual stress types on the final microstructure of CX after its heat treatment was studied. Samples were manufactured from fresh gas-atomized CX powder processed via an EOS M290 additive manufacturing system equipped with a 400 W Yb-Fiber laser. The specimens were manufactured in horizontal [loading axis (LA) \perp building direction (BD)] and vertical directions (LA \parallel BD), as shown in Figure 20 for the tensile and Charpy samples. Finally, the heat-treated specimens were post-processed following the temperature-time routines recommended by the powder manufacturer, shown in Figure 21 [1, 2].

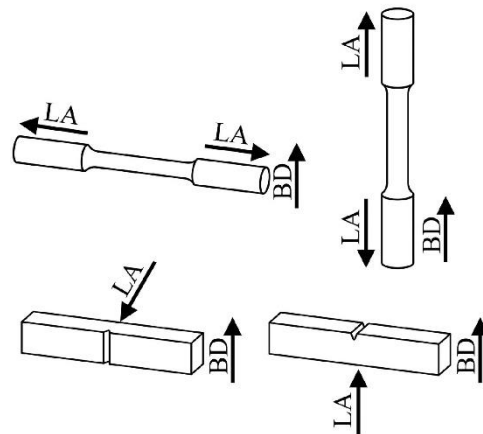


Figure 20. Schematic views of (left) horizontal and (right) vertical specimens [1].

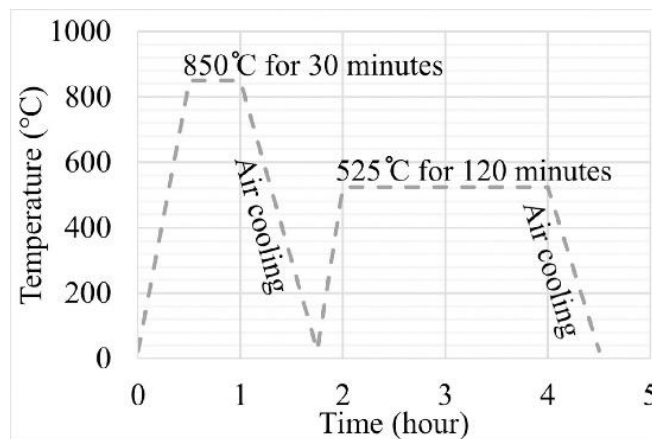


Figure 21. Time-temperature data of the heat treatment applied on some CX samples [1].

Results show that L-PBF CX had a martensitic microstructure in its as-built condition with minor amounts of retained austenite scattered along the high-angle grain boundaries, regardless of the building orientation (Figure 22). Quasi-static tensile tests showed that building the samples along the horizontal direction improved the material's mechanical performance under quasi-static loads, while machining did not show any significant positive effects (Table 10). Also, the heat treatment significantly improved the strength levels of the material, regardless of its building orientation and surface condition (machined or as built), while decreasing the ductility. The heat treatment also increased the Vickers hardness from ≈ 230 HV up to ≈ 470 HV [1, 2].

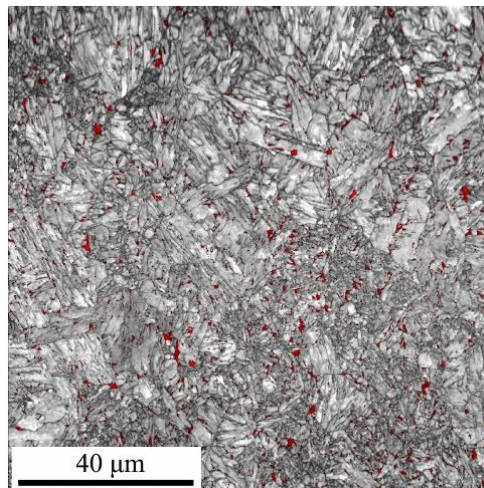


Figure 22. Microstructural image of the L-PBF CX showing retained austenite as red areas while the background is martensite [2].

Table 10. Mechanical properties of L-PBF CX [2].

Sample type	0.2% Yield strength (MPa)	Tensile strength (MPa)	Elongation (%)	Tangent modulus (GPa)
Machined horizontal (as-built)	1006.0	1170.4	16.6	197.8
Machined horizontal (heat-treated)	1533.4	1680.1	11.2	188.9
Raw vertical (as-built)	899.3	1081.2	13.3	175.7
Raw vertical (heat-treated)	1556.3	1641.5	8.1	194.5
Machined vertical (as-built)	919.2	1090.2	10.5	181.1
Machined vertical (heat-treated)	1600.9	1682.7	5.9	203.6

The mechanical performance of L-PBF CX under high-cycle fatigue loads was investigated as the next step. According to the results, surface quality (roughness) was the most determining factor influencing the fatigue life of L-PBF CX, as shown in Figure 23. Further, the simultaneous effect of applying the heat treatment and building the samples in the more favorable direction (horizontal) had a negligible effect on the fatigue performance of the material compared to the influence of the surface quality. Finally, to analyze the fatigue behavior via mathematical models, Murakami equations were used to estimate the fatigue life of L-PBF CX based on its surface and subsurface defects, similar to those shown in Figure 24. The results showed that samples with machined surfaces and the highest surface quality best fit the theoretical estimations using Murakami equations [3].

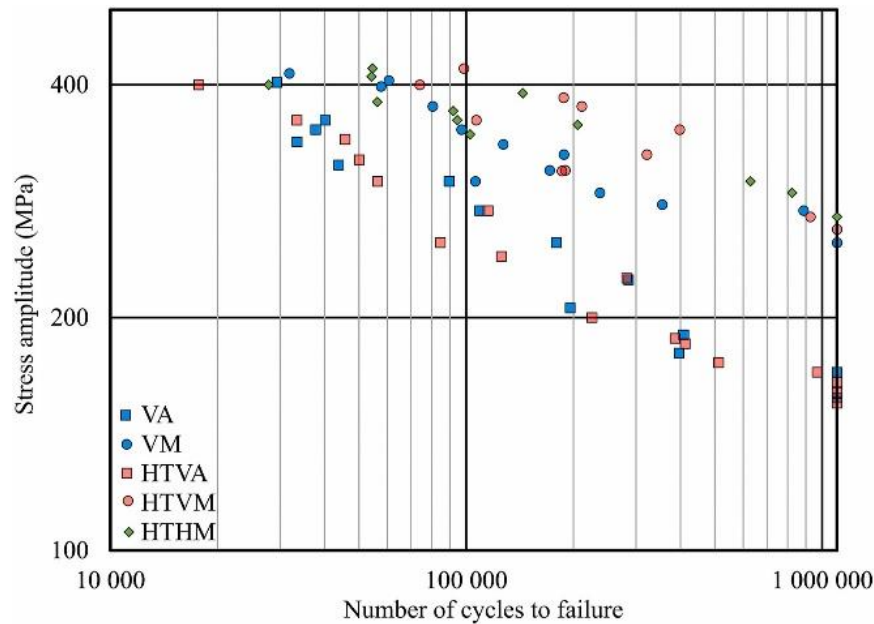


Figure 23. Fatigue lives L-PBF CX according to its manufacturing procedure (VA: vertically made with an as-built surface; VM: vertically made with a machined surface; HTVA: vertically made with as-built surface and heat-treated; HTVM: vertically made with machined surface and heat treated; HTHM: horizontally made with machined surface and heat-treated) [3].

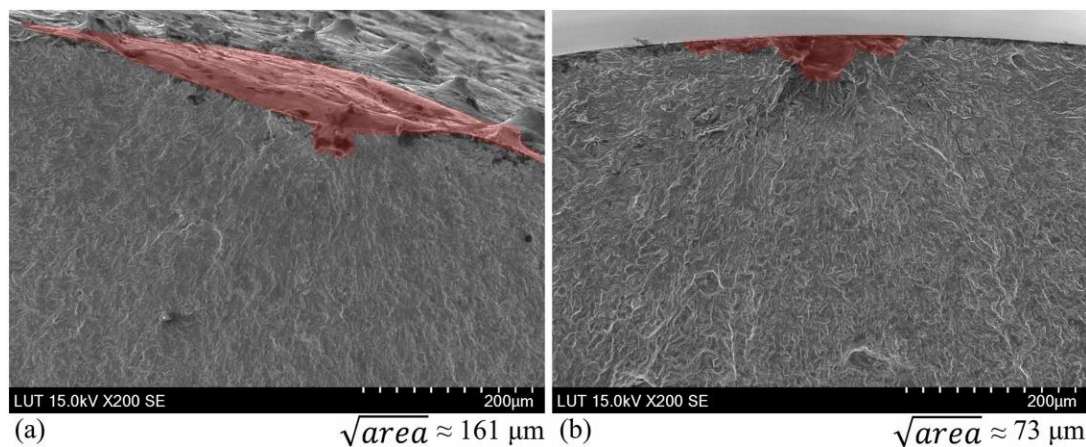


Figure 24. Critical defects caused the fatigue fracture of samples that are (a) vertically built with an as-built surface and (b) vertically built with a machined surface [3].

3.7 Notch-load interactions in L-PBF 18Ni300 and their effects on the mechanical performance of the material

Design optimizations and the ability to fabricate metal components with intricate geometrical features are among the most significant advantages of additive manufacturing as a fabrication method. However, introducing such complex geometrical features in mechanical design makes it impossible to avoid gradual to sudden changes in the cross-sections, areas, and angles throughout components. Hence, it is quite likely for such features

to act as geometrical notches under external loads. Further, metal fabricated via additive manufacturing, especially L-PBF, suffer from inherent defects. Consequently, the interactions between mentioned potential geometrical notches, inherent defects, and external loads can result in unexpected fracture behaviour and catastrophic failures in additively manufactured metallic components. Therefore, this study focused on ten different notch designs consisting of internal, external, sharp, blunt, V-shaped, and circular notches, as shown in Figure 25, to comprehensively investigate the influence of these notches on the mechanical performance of additively manufactured 18Ni300 under quasi-static and cyclic loads.

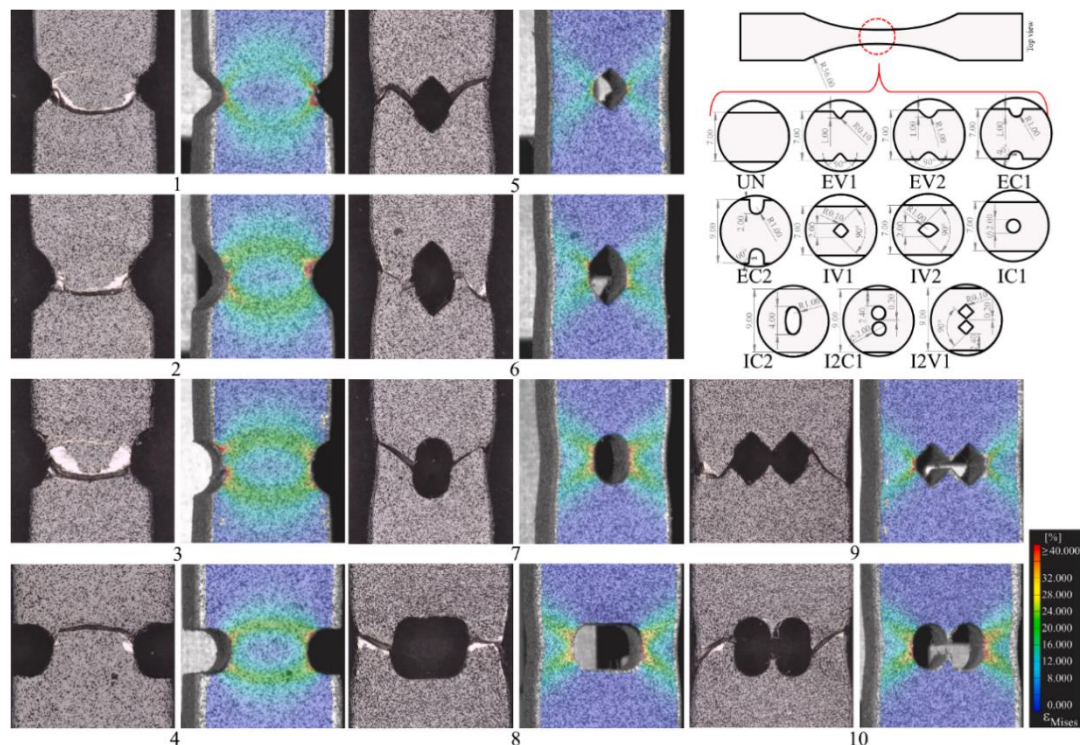


Figure 25. Schematics of notch designs (top right), their strain flows before their fracture under quasi-static uniaxial tensile loads (contour images achieved via digital image correlation), and their actual image after their fracture [4].

Results from the mechanical tests showed that the presence of notches, based on their stress concentration factor, location, and shape, significantly affect the mechanical performance of the material both under the quasi-static uniaxial tensile loads and high-cycle fatigue scenarios, as shown in Figure 26 and Figure 27 for quasi-static and fatigue tests, respectively. In conclusion, according to the results, all the notch designs decreased the ductility but caused an increase the strength. The notch-strengthening effect can be attributed to the stress triaxiality and stress distribution along the notch roots. Also, a direct correlation between the stress concentration factor and the magnitude of the strengthening was observed. Finally, all the fatigue samples failed from the surface defects inherent to L-PBF (Figure 28). Hence, surface roughness and other surface and subsurface defects dominated the fatigue performance of the samples, in addition to the geometrical notches.

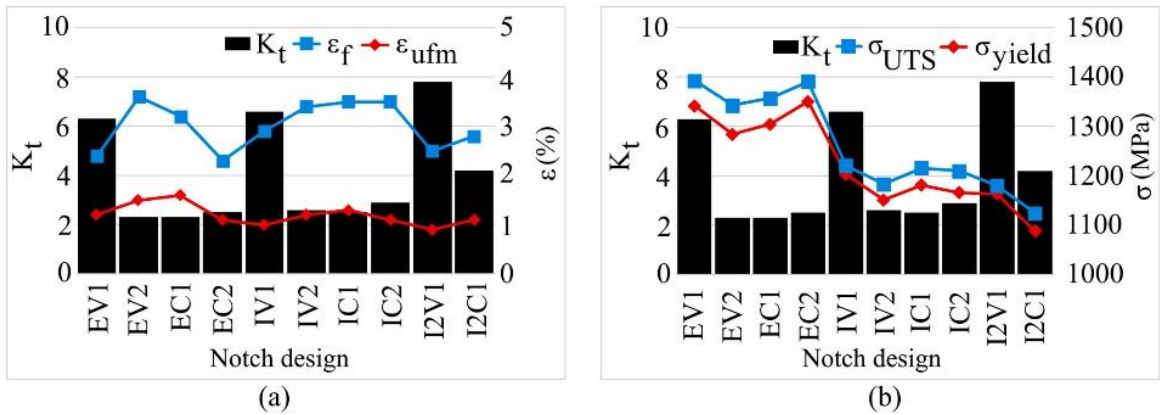


Figure 26. Variations in the ductility (ϵ_f), uniform elongation (ϵ_{ufm}), yield strength (σ_{yield}), and tensile strength (σ_{UTS}) according to the notch designs and their stress concentrations (K_t) [4].

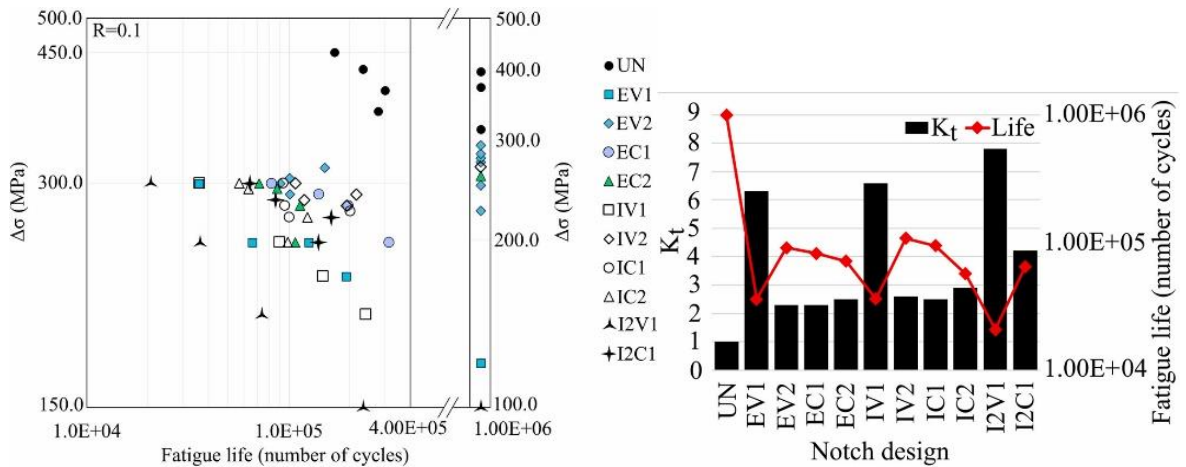


Figure 27. (left) stress-life data of the material from the high-cycle fatigue tests; and (b) comparison of the fatigue lives under the constant stress range of 300 MPa [4].

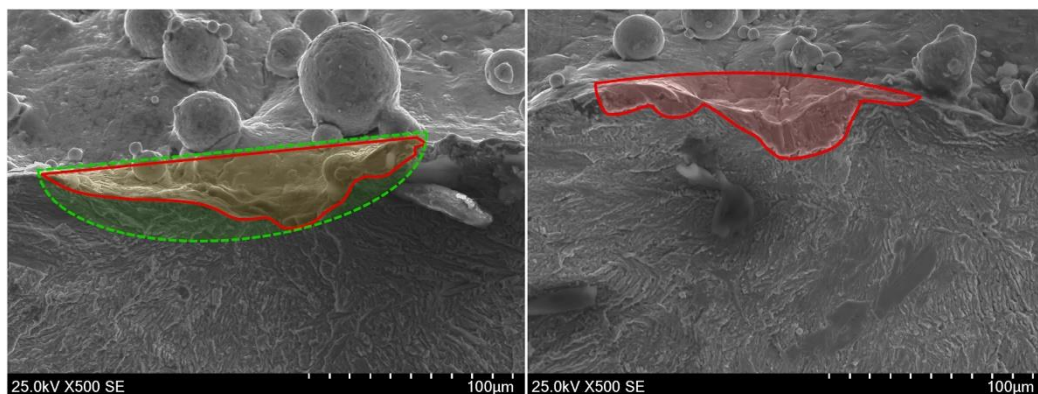


Figure 28. Critical defects in the samples with the sharp external V-notch failed under (left) maximum and (right) minimum stress ranges [4].

3.8 Mechanical performance and design optimization of additively manufactured honeycombs

Hollow sections have an essential presence comprising various industrial (e.g., aeronautics, aerospace, and automobile), constructional (i.e., civil and architecture), and medical applications. Honeycombs, as a type of hollow section, are widely utilized for passive protection in crash-worthy components and structures, especially in automobiles and aeronautics. The applicability of honeycombs for passive protection is because they are highly energy-absorbant and low in density. Furthermore, thanks to additive manufacturing, many opportunities are available for design optimization and integrating novel ideas into the classic concept of hollow structures, including honeycombs. Such modifications and changes can result in significant improvements in the characteristics and performance of these structures, ultimately resulting in their broader applicability. Consequently, this study investigates the application of L-PBF as a typically used additive manufacturing technique for industrial applications for producing metal honeycombs. Further, the applicability of stainless tool steel CX as a relatively new metal powder introduced to the market for fabricating reliable metal honeycomb is investigated.

Three typical hexagonal cell designs (A, B, and C in Figure 29) were considered to identify the most influential characteristics of additively manufactured honeycombs in this research. Furthermore, three modified designs (D, E, and F in Figure 29), which were only possible to manufacture via additive manufacturing, were included in this study to provide a comparison between the modified and classic cell designs. First, the build quality of the L-PBF honeycombs was evaluated based on their relative densities and dimensional accuracies, as shown in Figure 30. Next, the mechanical performance of the honeycombs was analyzed via quasi-static compressive loads and mechanical impacts (drop test); the tests were carried out along three principal axes (X, Y, and Z in Figure 29). Finally, the quasi-static test results were plotted as load-displacement graphs for quantitative comparisons (Figure 31, for example), while impact test results were presented as total distortions caused by impact loads (Figure 32, for example).

Finally, the finite element approach (Figure 33) and empirical equations were used to analyze the failure behavior of the honeycombs. In conclusion, the overall results showed that L-PBF could be considered a reliable method for fabricating metal honeycombs. However, limitations of the L-PBF technique for dimensional stability, accuracy, and surface roughness must be considered. Design modifications considered in this study significantly improved the mechanical performance of the honeycombs (Figure 34), either under quasi-static or impact loads. Furthermore, honeycombs with triangular cell designs (design E in Figure 29) outperformed those with hexagonal or diamond-shaped cells.

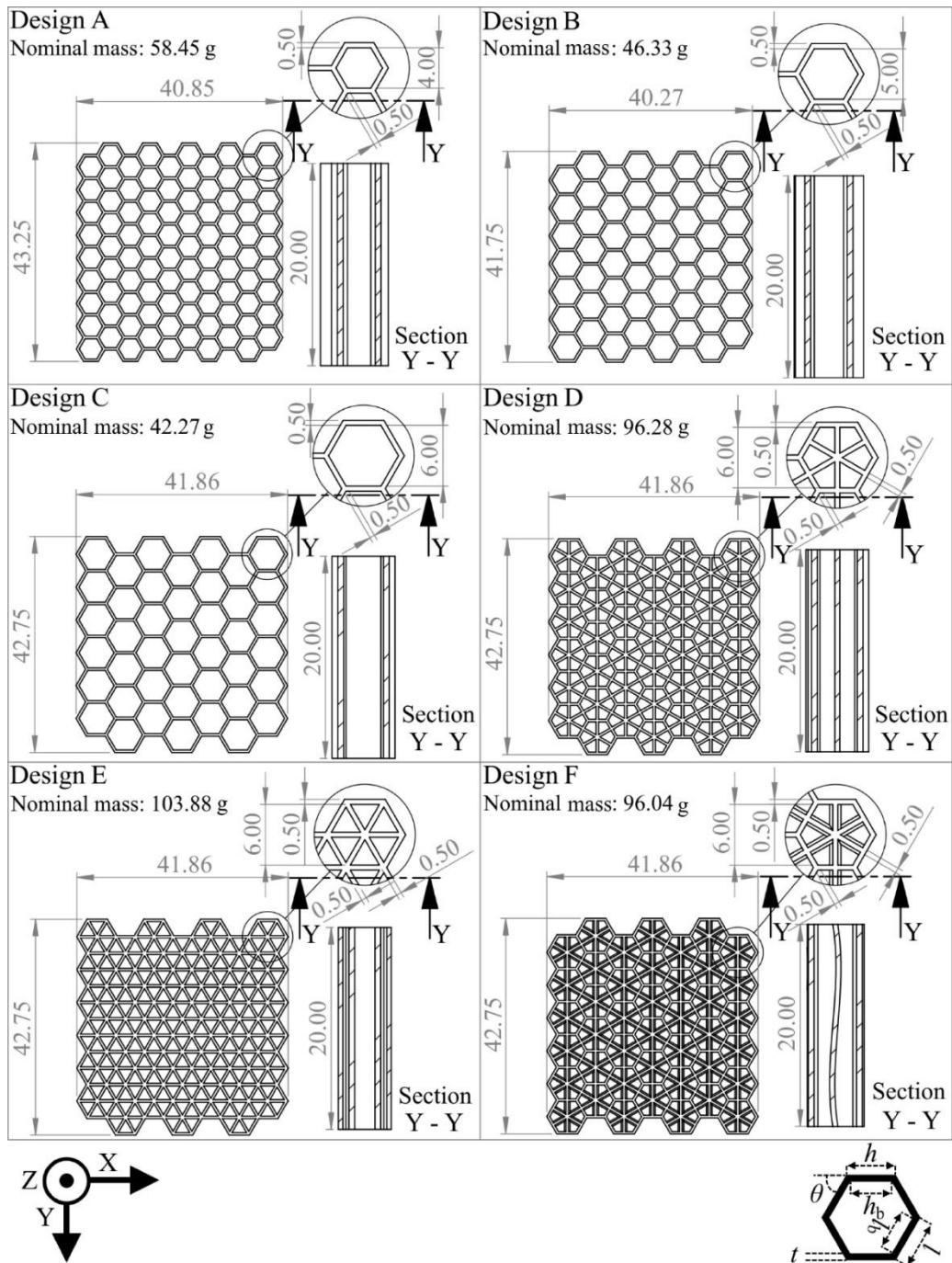


Figure 29. Honeycomb (cell) designs considered for the study [5, 6].

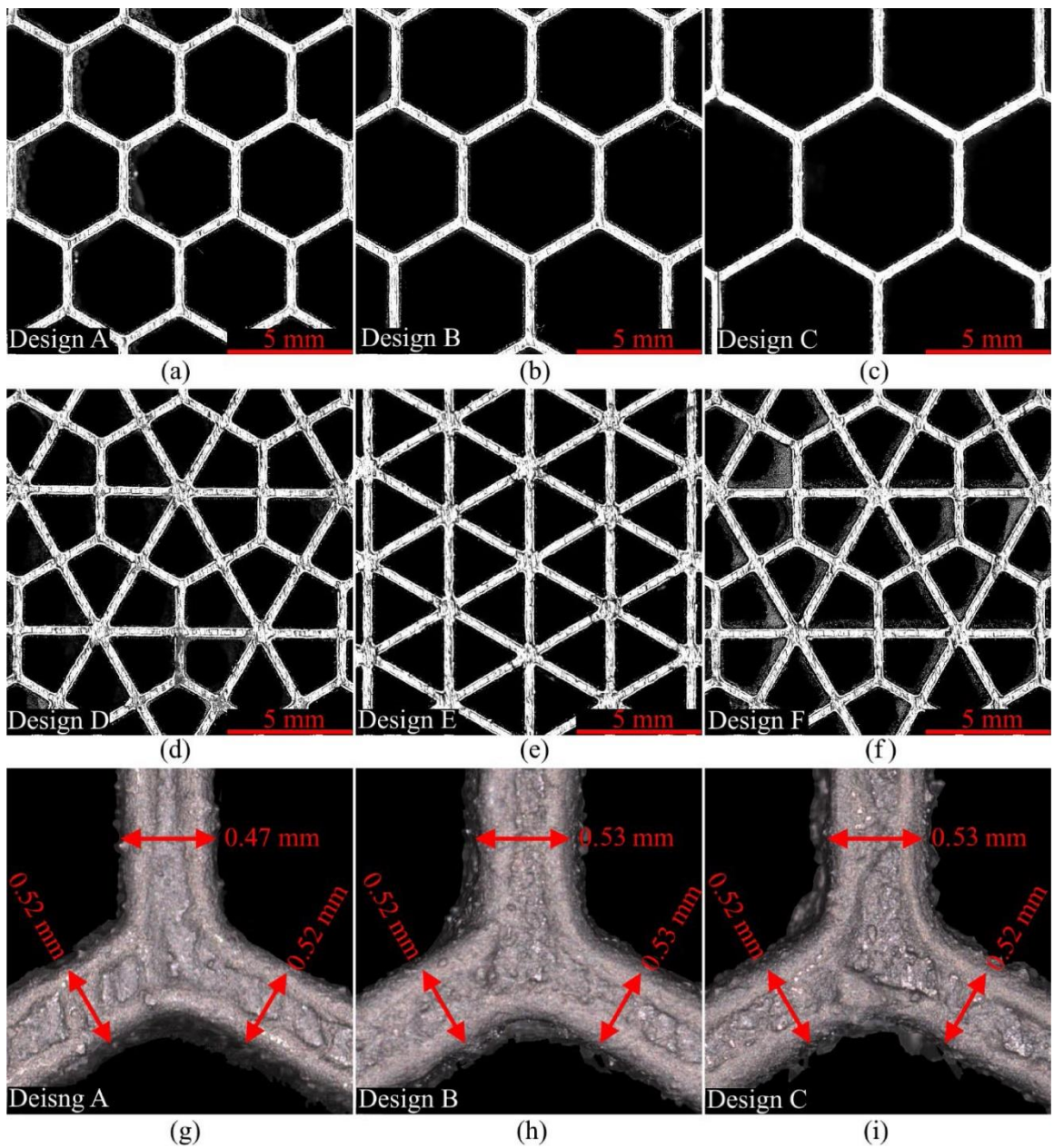


Figure 30. Frontal views of selected samples and dimensional accuracies achieved via L-PBF [5, 6].

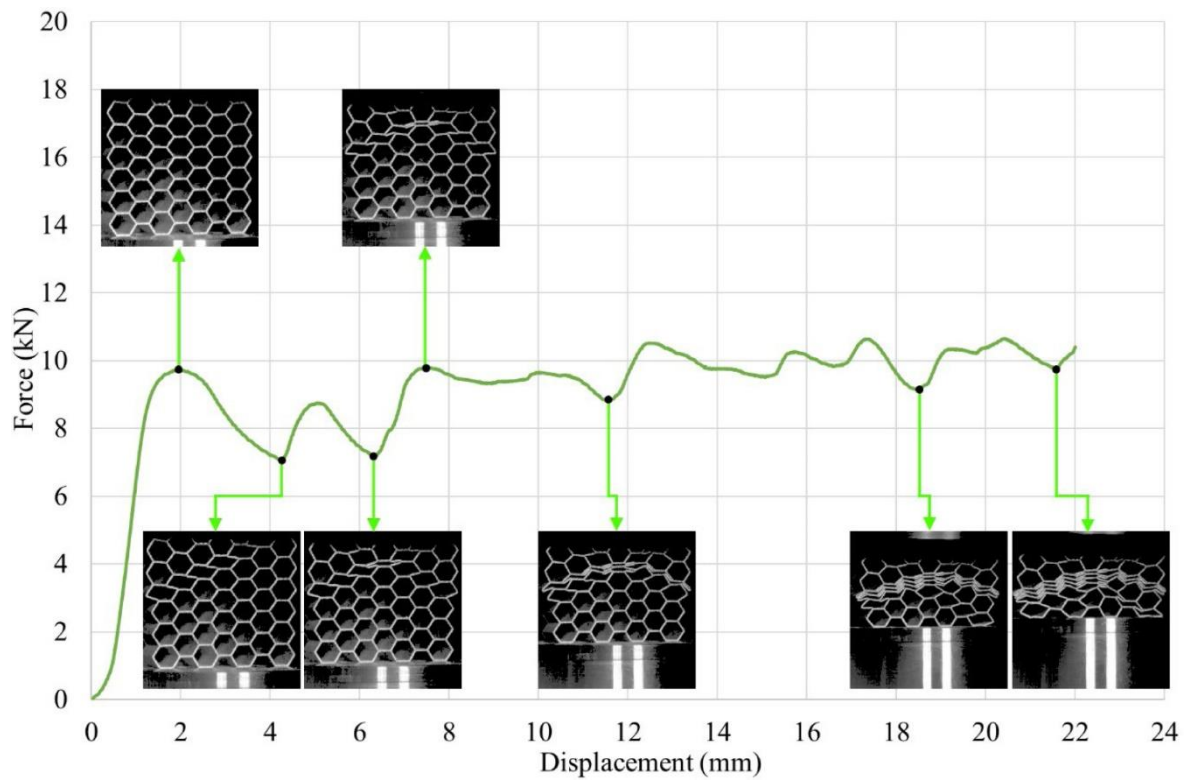


Figure 31. Load-displacement data of design C compressed along its Y direction [5, 6].

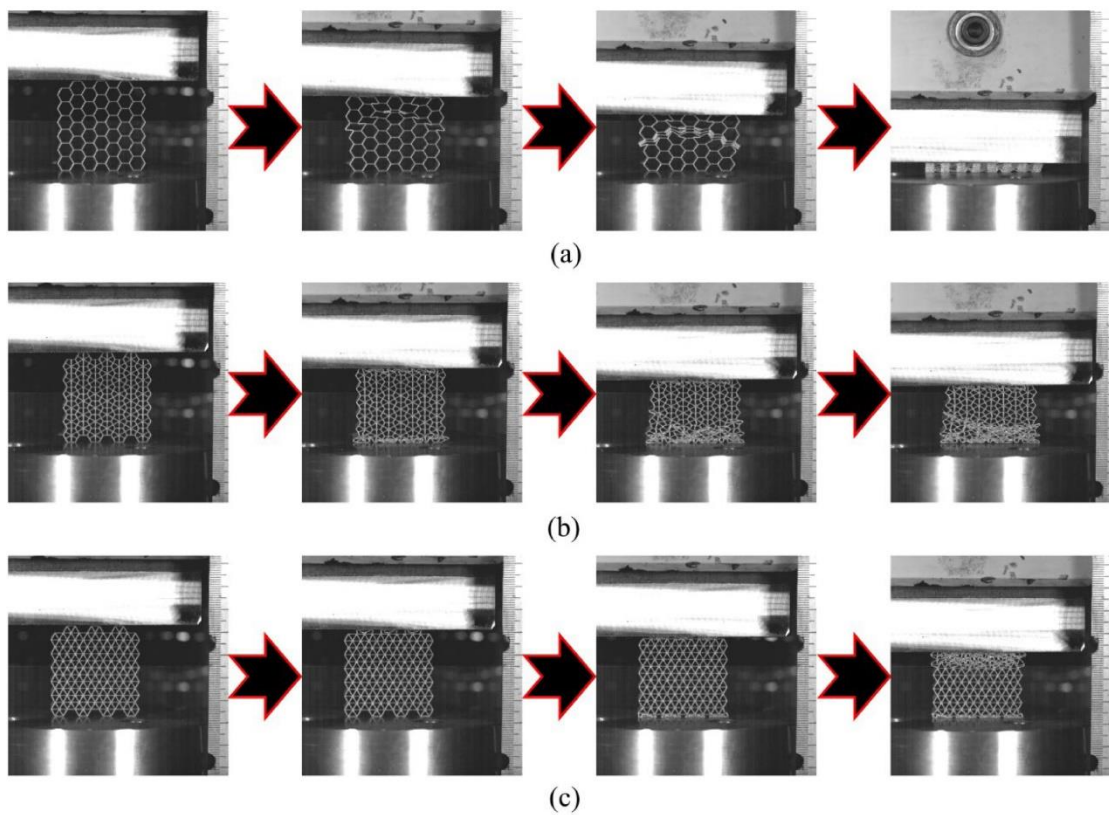


Figure 32. Impact (drop) test progress in three different honeycomb designs (A, D, and E) and their final displacements [5, 6].

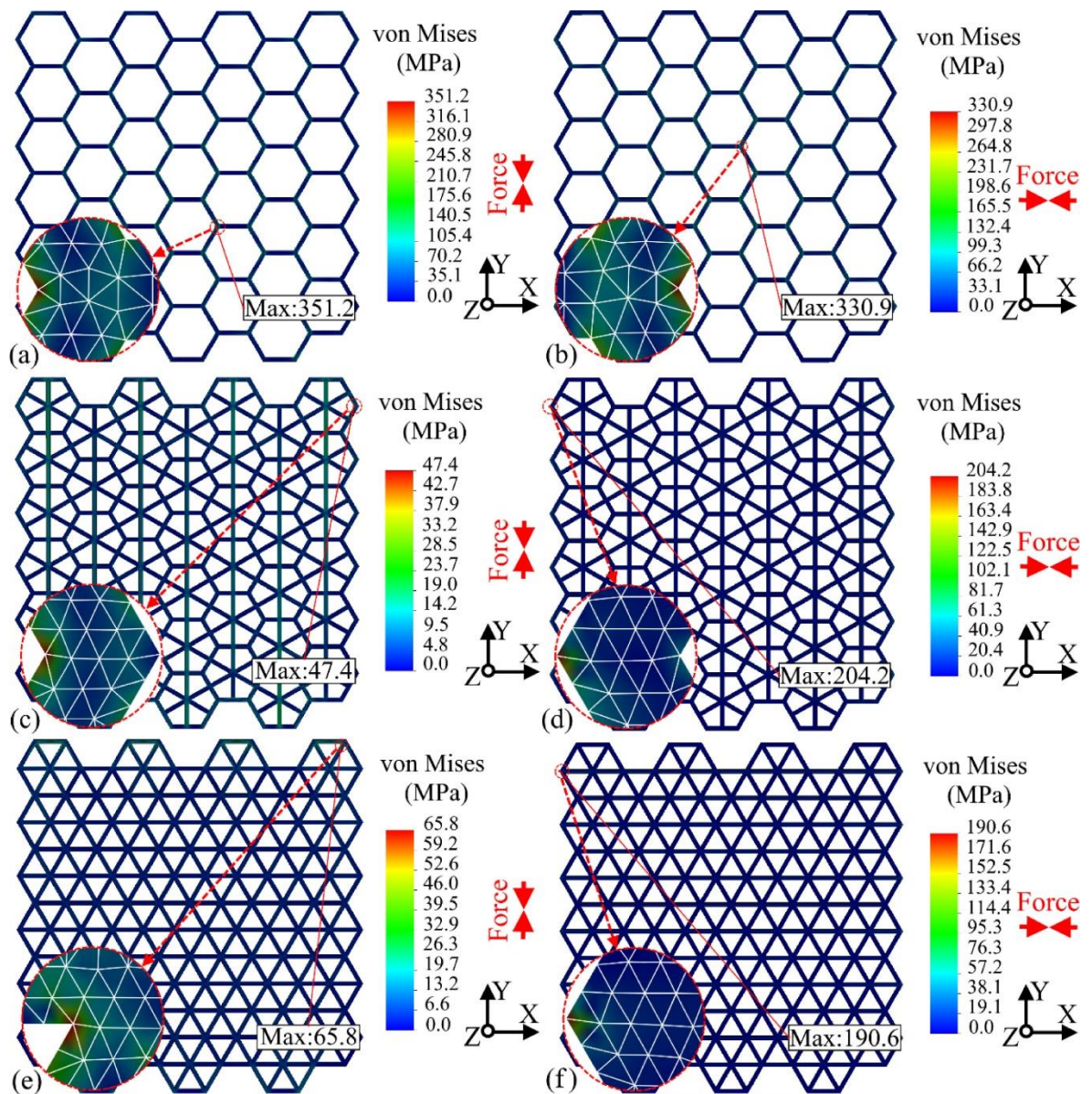


Figure 33. Finite element analysis of different honeycomb designs under equal elastic stress values to identify each design's stress concentration points and weak spots [5].

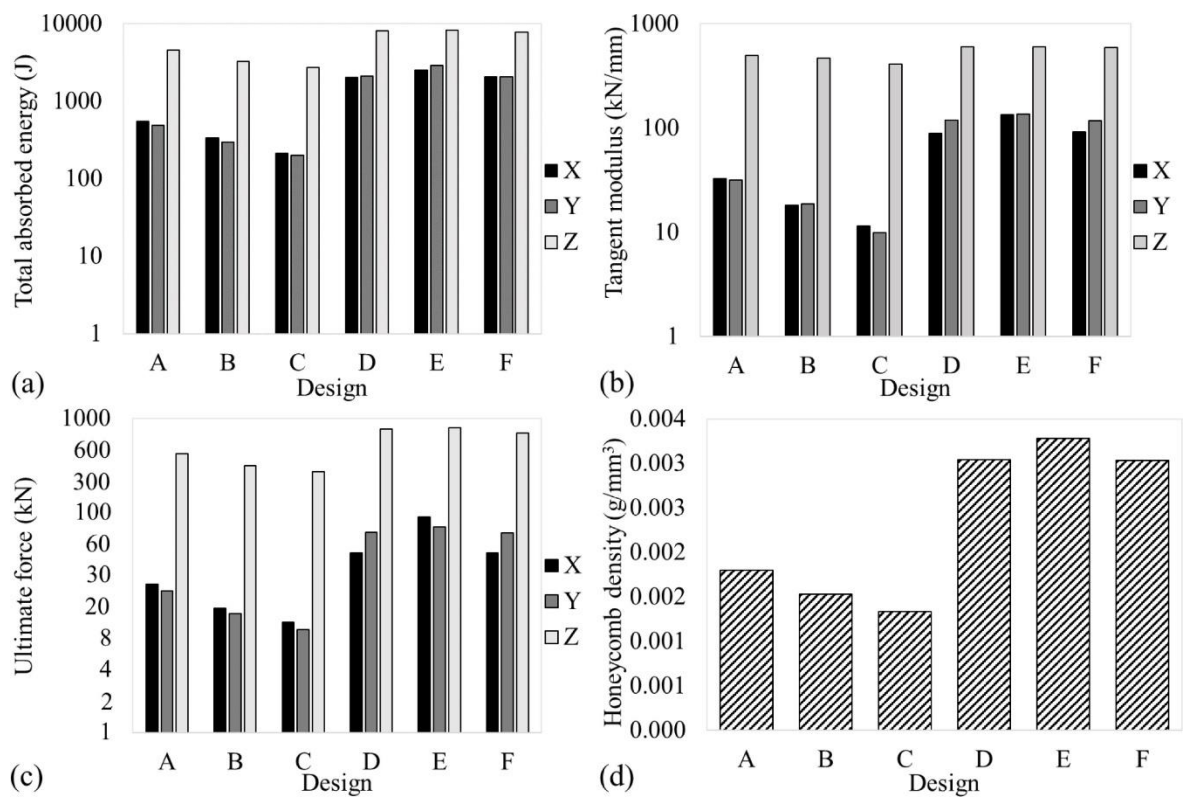


Figure 34. Comparing the mechanical performance of the honeycomb designs considered in this research [5].

4 Conclusions

In this project -Strength to Industrial 3D printing Via Networking and Research-VERKOTA, various steps were made to familiarize companies to metal 3D printing. In general companies have an interest in modern technologies. It was easy to find willing participants for steering such a project. During the project, many companies realized the efforts that are needed to design a new or redesign existing part for the AM. It can be also difficult to find a way to utilize full potential of additively manufactured parts. AM has its limitations, but often they could be overcome during design phase. Case studies showed that design phase can be done fast. Further improvement can also be made later with easy effort if needed.

There are some aspects in the utilization of AM that are still hindering the wider usage of the AM process. Two main reasons are the cost of the part and size limitations. The cost of the part can be high, but it can be compensated for total economy e.g., by repairing broken parts as in one case study. The solution for size limitation was addressed in this process by joining the AM parts with traditionally manufactured parts.

Material properties of the AM parts are also often questioned. These we extensively studied in this project. Mechanical properties are known to be good and in general there are not major things that are preventing the usage of metal AM parts even rigorous applications.

References

- [1] Afkhami S, Javaheri V, Dabiri E, Piili H, Björk T. Data related to the microstructural identification and analyzing the mechanical properties of maraging stainless steel 13Cr10Ni1. 7Mo2Al0. 4Mn0. 4Si (commercially known as CX) processed by laser powder bed fusion method. *Data in Brief*. 2022 Apr 1;41:107856.
- [2] Afkhami S, Javaheri V, Dabiri E, Piili H, Björk T. Effects of manufacturing parameters, heat treatment, and machining on the physical and mechanical properties of 13Cr10Ni1· 7Mo2Al0· 4Mn0· 4Si steel processed by laser powder bed fusion. *Materials Science and Engineering: A*. 2022 Jan 14;832:142402.
- [3] Afkhami S, Javaheri V, Lipiäinen K, Amraei M, Dabiri E, Björk T. Fatigue performance of stainless tool steel CX processed by laser powder bed fusion. *Materials Science and Engineering: A*. 2022 Apr 28;841:143031.
- [4] Afkhami S, Dabiri E, Lipiäinen K, Piili H, Björk T. Effects of notch-load interactions on the mechanical performance of 3D printed tool steel 18Ni300. *Additive Manufacturing*. 2021 Nov 1;47:102260.
- [5] Afkhami S, Amraei M, Gardner L, Piili H, Wadee MA, Salminen A, Björk T. Mechanical performance and design optimisation of metal honeycombs fabricated by laser powder bed fusion. *Thin-Walled Structures*. 2022 Nov 1;180:109864.
- [6] Afkhami S, Amraei M, Poutiainen I, Gardner L, Piili H, Wadee MA, Salminen A, Björk T. Data related to the manufacturing and mechanical performance of 3D-printed metal honeycombs. *Data in Brief*. 2023 Feb 1;46:108857.
- [7] Wohlers, T.T. *et al.* (2022) Wohlers report 2022: 3D Printing and Additive Manufacturing Global State of the industry. Fort Collins, CO: Wohlers Associates.

ISBN 978-952-335-954-3

ISSN-L 2243-3384

ISSN 2243-3384

Lappeenranta 2023

